

## Phase Fluctuations in a Strongly Disordered $s$ -Wave NbN Superconductor Close to the Metal-Insulator Transition

Mintu Mondal,<sup>1</sup> Anand Kamlapure,<sup>1,\*</sup> Madhavi Chand,<sup>1,†</sup> Garima Saraswat,<sup>1</sup> Sanjeev Kumar,<sup>1</sup> John Jesudasan,<sup>1</sup> L. Benfatto,<sup>2</sup> Vikram Tripathi,<sup>1</sup> and Pratap Raychaudhuri<sup>1,‡</sup>

<sup>1</sup>Tata Institute of Fundamental Research, Homi Bhabha Road, Mumbai 400005, India

<sup>2</sup>ISC-CNR and Department of Physics, Sapienza University, Piazzale Aldo Moro 5, 00185 Rome, Italy

(Received 27 June 2010; published 25 January 2011)

We explore the role of phase fluctuations in a three-dimensional  $s$ -wave superconductor, NbN, as we approach the critical disorder for destruction of the superconducting state. Close to critical disorder, we observe a finite gap in the electronic spectrum which persists at temperatures well above  $T_c$ . The superfluid density is strongly suppressed at low temperatures and evolves towards a linear- $T$  variation at higher temperatures. These observations provide strong evidence that phase fluctuations play a central role in the formation of a pseudogap state in a disordered  $s$ -wave superconductor.

DOI: 10.1103/PhysRevLett.106.047001

PACS numbers: 74.55.+v, 74.40.-n, 74.62.En, 74.70.Ad

Understanding the role of interaction and disorder is at the heart of understanding many-body quantum systems. Over the past few decades, it has been realized that the ground state in conventional superconductors, once thought to be resilient to disorder [1], gets destabilized at a critical value of disorder, giving rise to unusual metallic and insulating states [2,3]. However, recent experiments indicate that even after the global superconductivity is destroyed, the material continues to possess some of the fundamental properties commonly associated with the superconducting state. These include the dramatic observation of magnetic flux quantization in disorder driven insulating Bi films [4], finite high-frequency superfluid stiffness above  $T_c$  in amorphous InO<sub>x</sub> films [5], and the formation of a “pseudogapped” state [6] above  $T_c$  characterized by a finite gap in the electronic spectrum. Recent theoretical investigations [7] also indicate that strong superconducting correlation can persist even after global superconductivity is destroyed.

The superconducting state is characterized by a complex order parameter of the form  $\Psi = |\Delta|e^{i\phi}$  where three kinds of excitations can ultimately destroy the superconducting order: (i) quasiparticle excitations (QE) which primarily affect the amplitude  $|\Delta|$ ; (ii) quantum phase fluctuations (QPF) associated with the number-phase uncertainty relation; and (iii) classical phase fluctuations (CPF) caused by thermal excitations. In “clean” conventional superconductors, it is sufficient to consider QE alone [8], which are well described by Bardeen-Cooper-Schrieffer (BCS) and Eliashberg mean-field theories [9]. However, strongly disordered superconductors are characterized by poor screening of the Coulomb interactions [10] and small superfluid density ( $n_s$ ) due to disorder scattering [9], making them susceptible to phase fluctuations. Since strong phase fluctuations can destroy the global superconducting order well before  $|\Delta|$  goes to zero, a larger role of phase fluctuations could explain the persistence of superconducting

properties above  $T_c$ . Numerical simulations [11] also show that the superconducting state can get destroyed by strong phase fluctuations between domains that emerge in the presence of strong disorder.

In this Letter, we explore the role of phase fluctuations in strongly disordered superconducting NbN films, using a combination of scanning tunneling spectroscopy (STS) and penetration depth ( $\lambda$ ) measurements. The effective disorder, characterized by the product of Fermi wave vector ( $k_F$ ) and electronic mean free path ( $l$ ), ranges from  $k_F l \sim 1.24$ – $10.12$ . In this range,  $T_c$  (the temperature where the resistance reaches 1% of its normal state value) decreases from 16.8 K to  $<300$  mK. In films with  $T_c \lesssim 6$  K, we observe that the dip in the tunneling density of states (DOS) associated with the superconducting energy gap ( $\Delta$ ), persists well above  $T_c$ ; on the other hand  $n_s \propto \lambda^{-2}$  is suppressed compared to the BCS estimate, and shows a gradual evolution towards linear temperature variation. These observations provide compelling evidence of the role of phase fluctuations in a strongly disordered  $s$ -wave superconductor.

Our samples consist of epitaxial NbN films grown through reactive magnetron sputtering on single crystalline MgO substrates, with thickness  $\geq 50$  nm, which is much larger than the dirty-limit coherence length ( $\xi \sim 4$ – $8$  nm) [12]. The disorder in these films can be tuned by controlling the level of Nb vacancies in the NbN crystalline lattice, which is controlled by controlling the Nb/N ratio in the plasma [13,14].  $k_F l$  is determined from the resistivity ( $\rho$ ) and Hall coefficient ( $R_H$ ) using the free electron formula  $k_F l = \{(3\pi^2)^{2/3} \hbar [R_H(285 \text{ K})]^{1/3}\} / [\rho(285 \text{ K}) e^{5/3}]$  ( $\hbar$  is Planck’s constant and  $e$  is the electronic charge). The absolute value of  $\lambda$  is measured using a low-frequency (60 kHz) two coil mutual inductance technique [15] on 8 mm diameter circular films patterned using a shadow mask. The temperature dependence of the tunneling-DOS is probed from the measurement of tunneling conductance

$[G(V) = (dI/dV)|_V]$  using an *in situ*, high-vacuum, low-temperature scanning tunneling microscope [16] (STM) operating down to 2.6 K. Tunneling measurements were also performed on disordered NbN/insulator/Ag planar tunnel junctions [17] at 500 mK in a  $^3\text{He}$  cryostat.

Figure 1(a) shows the conductivity ( $\sigma$ ) as a function of temperature for a series of NbN films. While most of the films display  $(d\sigma/dT) > 0$  in the normal state [14], even in the most disordered film [inset (a)], the variation in  $\sigma$ - $T$  (after superconductivity is suppressed by the application of a magnetic field) clearly suggests that  $\sigma(T \rightarrow 0) \neq 0$ . Therefore, all of our samples are on the metallic side of the Anderson metal-insulator transition (MIT). Figure 1(b) shows that both the conductivity just before the onset of the superconducting transition ( $\sigma_0$ ) and  $T_c$  asymptotically go to zero as  $k_F l \rightarrow 1$ . Therefore, the critical disorder for destruction of superconductivity coincides with the MIT. While a direct transition from a superconducting to an insulating state with disorder is ubiquitous in ultrathin two-dimensional films [2], in 3D, both superconductor-normal metal and superconductor-insulator transitions have been observed and theoretically predicted [10,18,19]. At present, we do not know whether this coincidence, similar to that reported for 3D boron-doped diamond epitaxial films [20], is merely accidental.

The temperature evolution of the tunneling DOS was investigated through STS measurements performed on several samples with different disorder. Figures 2(a)–2(c) show the temperature dependence of the tunneling DOS in the form of an intensity plot [16] of the normalized conductance  $G(V)/G_N$  [where  $G_N = G(V \gg \Delta/e)$ ], as a function of temperature and bias voltage for three different films. For each temperature, the  $G(V)$  vs  $V$  spectrum is spatially averaged over 32 points taken at equal intervals along a 150 nm line. The resistance vs temperature for each sample is shown in the same panel. At the lowest temperature,  $G(V)/G_N$  vs  $V$  for the first two samples (shown in inset) show a dip close to  $V = 0$  and two symmetric peaks, as expected from BCS theory. For the sample with

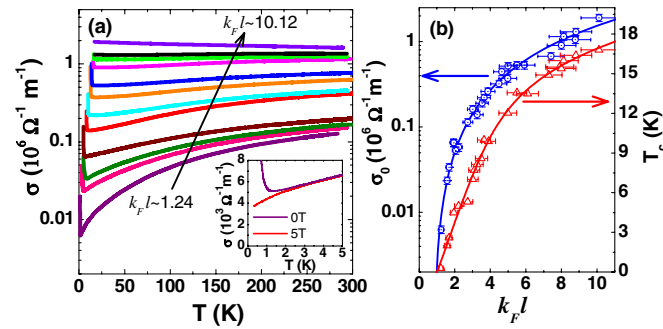


FIG. 1 (color online). (a)  $\sigma$  vs  $T$  for films with  $k_F l \sim 10.12, 8.82, 8.13, 8.01, 5.5, 4.98, 3.65, 3.27, 2.21, 1.68, 1.58,$  and  $1.24$ . The inset shows an expanded view of  $\sigma(T)$  for the film with  $k_F l \sim 1.24$  in zero field and in magnetic field of  $5T$ . (b)  $\sigma_0$  and  $T_c$  as a function of  $k_F l$ .

$T_c \sim 11.9$  K, a flat metallic DOS is restored for  $T > T_c$ . However, with increase in disorder a pseudogapped phase emerges, where the dip in the DOS persists above  $T_c$ . In the most disordered sample ( $T_c \sim 1.65$  K), the pseudogap persists well beyond the onset of the superconducting transition, up to  $\sim 6.5$  K. We would also like to note that even above the pseudogap temperature, in all our samples, a “V” shape in the  $G(V)/G_N$  spectra [21] extends up to  $V \gg \Delta/e$ . This feature, which is not associated with superconductivity, arises from Altshuler-Aronov (AA) type interactions in the normal state. To extract the pseudogap feature associated with superconductivity in the most disordered sample ( $T_c \sim 1.65$  K), we subtract the AA background using the spectra obtained at 8 K [22], from the spectra obtained at 2.65 K. The resulting curve

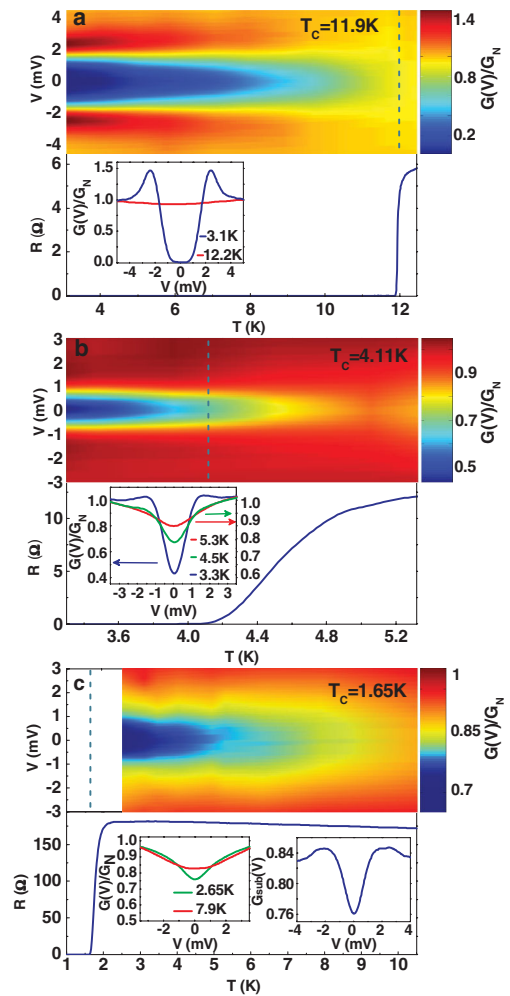


FIG. 2 (color). (a)–(c) Intensity plots of  $G(V)/G_N$  as a function of temperature and applied bias for three different films (upper panels), and the resistance vs temperature ( $R$ - $T$ ) in the same temperature range (lower panels); vertical dotted lines in the upper panels correspond to  $T_c$ . Insets of panels (a), (b) and left inset of panel (c) show representative tunneling spectra in the superconducting state (blue), in the pseudogap state (green) and above the pseudogap temperature (red). The right inset of panel (c) shows the AA background subtracted spectra at 2.65 K.

$G_{\text{sub}}(V) = \{ [G(V)/G_N] |_{T=2.65 \text{ K}} - [G(V)/G_N] |_{T=8 \text{ K}} + 0.76 \}$  [right inset of Fig. 2(c)] clearly reveals the presence of broadened coherence peaks around 2 mV confirming the superconducting origin of the pseudogap feature. In addition, the individual line scans [23], reveal that the superconducting state becomes progressively inhomogeneous as the disorder is increased [11].

To investigate the origin of the ‘‘pseudogap’’ behavior we now focus on  $\lambda(T)$ .  $\lambda^{-2}(T) \propto n_s$  [ $\equiv m^*/(\mu_0 e^2 \lambda^2)$ , where  $m^*$  is the effective mass of the electron], gets strongly renormalized [24,25] in the presence of phase fluctuations. Figures 3(a) and 3(b) show the temperature variation of  $\lambda^{-2}(T)$  in a series of NbN films with different  $T_c$ . At low disorder the temperature variation agrees well with the dirty-limit BCS expression [9],  $\lambda^{-2}(T)/\lambda^{-2}(0) = \{\Delta(T)/\Delta(0)\} \tanh[\Delta(T)/(2k_B T)]$ , where  $k_B$  is the Boltzman constant. However, as disorder increases two effects become noticeable: (i)  $\lambda^{-2}(T \rightarrow 0)$  decreases rapidly by 2 orders of magnitude and (ii)  $\lambda^{-2}(T)$  decreases faster than the expected BCS temperature variation. First we concentrate on  $\lambda^{-2}(T \rightarrow 0)$ . In the absence of phase fluctuations,  $\lambda^{-2}(0)$  is reduced by disorder scattering according to the BCS relation [9],  $\lambda^{-2}(0)_{\text{BCS}} = \pi \mu_0 \Delta(0) \sigma_0 / \hbar$ . For NbN, we find  $\Delta(0) \approx 2.05 k_B T_c$  from tunneling measurements performed at low temperatures ( $T < 0.2 T_c$ ) on planar tunnel junctions fabricated on a number of samples with different disorder [26] [inset Fig. 3(c)]. Figure 3(c) shows that  $\lambda^{-2}(0) \approx \lambda^{-2}(0)_{\text{BCS}}$  within experimental error for samples with  $T_c > 6$  K. However, as we approach the critical disorder  $\lambda^{-2}(0)$  becomes gradually smaller than  $\lambda^{-2}(0)_{\text{BCS}}$ , reaching a value which is 50% of  $\lambda^{-2}(0)_{\text{BCS}}$  for the sample with  $T_c \sim 2.27$  K. Also, while in all samples  $\lambda^{-2}(T)$  saturates

as  $T \rightarrow 0$ , at higher temperatures, samples with  $T_c < 6$  K show a gradual evolution towards a linear- $T$  variation. This is most clearly observed in the sample with  $T_c \sim 2.27$  K [Fig. 3(d)].

Since the suppression of  $\lambda(0)^{-2}$  from its BCS value and linear- $T$  dependence of  $\lambda^{-2}(T)$  are characteristic features associated with QPF and CPF [27], respectively, we now try to quantitatively analyze our data. The importance of QPF and CPF is determined by two energy scales [8]: the Coulomb energy  $E_c$ , and the superfluid stiffness  $J$ , which can be estimated for a 3D superconductor from the relations [25],  $E_c = (16\pi e^2)/(\varepsilon_\infty a)$  and  $J = (\hbar^2 a n_s)/(4m^*)$ , where  $\varepsilon_\infty$  is the background dielectric constant and  $a$  is the characteristic length scale for phase fluctuations. The suppression of  $\lambda^{-2}(0)$  from QPF can be estimated using the self-consistent harmonic approximation [28] which predicts (in 3D),  $n_s(T=0)/n_{s0}(T=0) = e^{-\Delta\theta^2(T=0)/6}$  ( $n_{s0}$  is the bare value in the absence of phase fluctuations), where  $\Delta\theta^2(T=0) = (1/2)\sqrt{E_c/J}$ . At the same time, the energy scale above which phase fluctuations become classical is given by the Josephson plasma frequency ( $\hbar\omega_p = \sqrt{4\pi e^2 n_s/m^* \varepsilon_\infty} = \sqrt{E_c J}$ ). We calculate these values for the sample with  $T_c \sim 2.27$  K. For NbN, we estimate  $\varepsilon_\infty \approx 30$  from the plasma frequency ( $12600 \text{ cm}^{-1}$ ) measured [29] at low temperatures. Taking  $a \approx \xi \sim 8$  nm (Ref. [12]), we obtain  $E_c \approx 0.3$  eV and  $J \approx 0.14$  meV at  $T = 0$ , corresponding to  $n_s(T=0)/n_{s0}(T=0) \approx 0.02$ . While this value is likely to have some inaccuracy due to the exponential amplification of errors in our estimate of  $E_c$  or  $J$ , the important point is that this suppression is much larger than our experimental estimate,  $\lambda^{-2}(0)/\lambda_{\text{BCS}}^{-2}(0) \approx 0.5$ . On the other hand  $\hbar\omega_p \sim 6.5$  meV  $\equiv 75$  K, so that one should conclude that CPF cannot be responsible for the observed linear temperature dependence of  $\lambda^{-2}(T)$  in this sample.

These two apparent contradictions can be resolved by considering the role of dissipation. In  $d$ -wave superconductors, the presence of low energy dissipation has been theoretically predicted [30] and experimentally observed from high-frequency conductivity [31,32] measurements. Recent measurements [33] on amorphous  $\text{InO}_x$  films reveal that low energy dissipation can also be present in strongly disordered  $s$ -wave superconductors [34]. While the origin of this dissipation is not clear at present, the presence of dissipation has several effects on phase fluctuations [25]: (i) QPF are less effective in suppressing  $n_s$ ; (ii) QPF contribute to a  $T^2$  temperature depletion of  $n_s$  of the form  $n_s/n_{s0} = 1 - BT^2$  at low temperature where  $B$  is directly proportional to the dissipation, and (iii) the crossover to the usual linear temperature dependence of  $n_s$  due to CPF,  $n_s/n_{s0} = 1 - (T/6J)$ , occurs at a characteristic temperature that is much smaller than  $\hbar\omega_p/k_B$ , and scales approximately as  $T_{cl} \approx J/\bar{\sigma}$ , where  $\bar{\sigma}$  is a dimensionless measure of the residual conductivity in the SC state. In the sample with  $T_c \sim 2.27$  K, the  $T^2$  variation of  $\lambda(T)^{-2}/\lambda(0)^{-2}$  can be clearly resolved [15] below 650 mK [inset, Fig. 3(d)].

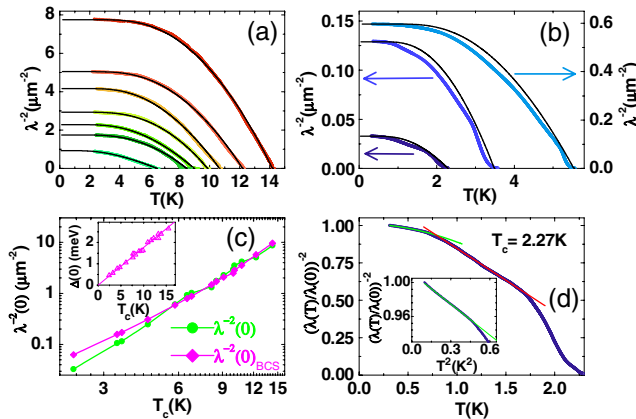


FIG. 3 (color online). (a),(b)  $\lambda^{-2}(T)$  for NbN films with different disorder; the solid lines are the expected temperature variation from dirty-limit BCS theory. (c)  $\lambda^{-2}(0)$  and  $\lambda^{-2}(0)_{\text{BCS}}$  as function of  $T_c$ ; the inset shows the variation  $\Delta(0)$  as function of  $T_c$ . (d) Temperature variation of  $[\lambda(T)/\lambda(0)]^{-2}$  for the film with  $T_c = 2.27$  K; the solid lines are fits to the  $T^2$  dependence of  $\lambda^{-2}(T)/\lambda^{-2}(0)$  at low temperature ( $T \leq 0.65$  K) and the  $T$  dependence at higher temperature; the inset shows an expanded view of the  $T^2$  dependence at low temperatures.

In the same sample, the slope of the linear- $T$  region is 3 times larger than the slope estimated from the value of  $J$  calculated for  $T = 0$ . This discrepancy is, however, minor considering the approximations involved. In addition, at finite temperatures  $n_{s0}$  gets renormalized due to QE. With decrease in disorder, QE eventually dominates over the phase fluctuations, thereby recovering the usual BCS temperature dependence at low disorder. The increased role of CPF could naturally explain the observation of a pseudogapped state in strongly disordered NbN films. We would also like to note that in all the disordered samples  $\lambda^{-2}(T)$  shows an abrupt downturn close to  $T_c$ , reminiscent of the Kosterlitz-Thouless (KT) transition [15]. However, since in 3D a KT transition is not expected, we do not know the origin of this behavior.

To summarize, we observe a progressive increase in phase fluctuations and the formation of a pseudogap state in strongly disordered NbN thin films. These observations support the scenario where the superconducting transition is governed by phase disordering. The remaining question is on the role of amplitude fluctuations arising from non-equilibrium Cooper pairs, which can also produce a dip in the tunneling DOS above  $T_c$ . While our experiments cannot rule out the possibility of amplitude fluctuations also playing a role [35], within a standard Ginzburg-Landau (G-L) approach this effect is much smaller [36] than the pseudogap feature observed in our samples. However, it would be worthwhile to critically explore the applicability of conventional G-L theory close to the MIT to assess the role of amplitude fluctuations. It would also be interesting to use a comparative analysis between tunneling DOS and  $\lambda$  to understand the extent to which the pseudogap state in underdoped high- $T_c$  cuprates can be understood within a phase-fluctuations scenario.

We would like to thank T. V. Ramakrishnan, S. Mandal, and M. V. Feigelman for enlightening discussions and V. Bagwe and S. P. Pai for technical help.

---

\*ask@tifr.res.in

†chand@tifr.res.in

\*pratap@tifr.res.in

- [1] P. W. Anderson, *J. Phys. Chem. Solids* **11**, 26 (1959).  
 [2] A. M. Goldman and N. Marković, *Phys. Today* **51**, No. 11, 39 (1998).  
 [3] V. F. Gantmakher, *Theory of Quantum Transport in Metallic and Hybrid Nanostructures*, edited by A. Glatz *et al.* (Springer, New York, 2006), p. 83.  
 [4] M. D. Stewart *et al.*, *Science* **318**, 1273 (2007).  
 [5] R. Crane *et al.*, *Phys. Rev. B* **75**, 184530 (2007).  
 [6] B. Sacepe *et al.*, *Phys. Rev. Lett.* **101**, 157006 (2008); *Nature Commun.* **1**, 140 (2010).  
 [7] M. V. Feigelman *et al.*, *Phys. Rev. Lett.* **98**, 027001 (2007); *Ann. Phys. (N.Y.)* **325**, 1390 (2010).  
 [8] V. J. Emery and S. A. Kivelson, *Nature (London)* **374**, 434 (1995).  
 [9] M. Tinkham, *Introduction to Superconductivity* (McGraw-Hill, Singapore, 1996).  
 [10] A. M. Finkelstein, *Physica (Amsterdam)* **197B**, 636 (1994); P. W. Anderson, K. A. Muttalib, and T. V. Ramakrishnan, *Phys. Rev. B* **28**, 117 (1983).  
 [11] A. Ghosal, M. Randeria, and N. Trivedi, *Phys. Rev. Lett.* **81**, 3940 (1998); Y. Dubi, Y. Meir, and Y. Avishai, *Nature (London)* **449**, 876 (2007).  
 [12] M. Mondal *et al.*, *J. Supercond. Nov. Magn.* (in press).  
 [13] S. P. Chockalingam *et al.*, *Phys. Rev. B* **77**, 214503 (2008).  
 [14] M. Chand *et al.*, *Phys. Rev. B* **80**, 134514 (2009).  
 [15] A. Kamlapure *et al.*, *Appl. Phys. Lett.* **96**, 072509 (2010); see supplemental material at <http://link.aps.org/supplemental/10.1103/PhysRevLett.106.047001> for analysis of low temperature  $\lambda^{-2}(T)$  data, Sec. 4.  
 [16] See supplemental material at <http://link.aps.org/supplemental/10.1103/PhysRevLett.106.047001> for details of the STM, Sec. 1.  
 [17] S. P. Chockalingam *et al.*, *Phys. Rev. B* **79**, 094509 (2009).  
 [18] A. Kapitulnik and G. Kotliar, *Phys. Rev. Lett.* **54**, 473 (1985); M. Ma and P. A. Lee, *Phys. Rev. B* **32**, 5658 (1985).  
 [19] M. Ma and E. Fradkin, *Phys. Rev. Lett.* **56**, 1416 (1986).  
 [20] T. Klein *et al.*, *Phys. Rev. B* **75**, 165313 (2007).  
 [21] This is also observed in planar tunnel junctions [17].  
 [22] Since the AA background is weakly temperature dependent, we use the spectra taken at the lowest temperature where the low bias feature associated with superconductivity disappears to subtract the background.  
 [23] See supplemental material at <http://link.aps.org/supplemental/10.1103/PhysRevLett.106.047001> for individual line scans, Sec. 3.  
 [24] C. Ebner and D. Stroud, *Phys. Rev. B* **28**, 5053 (1983).  
 [25] L. Benfatto *et al.*, *Phys. Rev. B* **63**, 174513 (2001).  
 [26] This is in variance with Ref. [17] where an apparent increase of  $2\Delta/k_B T_c$  was reported for a much smaller range of disorder.  
 [27] E. Roddick and D. Stroud, *Phys. Rev. Lett.* **74**, 1430 (1995).  
 [28] S. Chakravarty *et al.*, *Phys. Rev. Lett.* **56**, 2303 (1986); *Phys. Rev. B* **37**, 3283 (1988).  
 [29] M. Tazawa *et al.*, *Int. J. Infrared Millim. Waves* **19**, 1155 (1998).  
 [30] P. A. Lee, *Phys. Rev. Lett.* **71**, 1887 (1993).  
 [31] S.-F. Lee *et al.*, *Phys. Rev. Lett.* **77**, 735 (1996).  
 [32] J. Corson *et al.*, *Phys. Rev. Lett.* **85**, 2569 (2000).  
 [33] R. W. Crane *et al.*, *Phys. Rev. B* **75**, 094506 (2007).  
 [34] See supplemental material at <http://link.aps.org/supplemental/10.1103/PhysRevLett.106.047001> for indirect evidence of low energy dissipation in our system obtained from low temperature tunneling DOS, Sec. 2.  
 [35] J. L. Tallon, J. G. Storey, and J. W. Loram, [arXiv:0908.4428](https://arxiv.org/abs/0908.4428).  
 [36] In the dirty limit, the dip in  $G(V)$  at  $V = 0$  is expected to be of the order of  $(\delta G/G)_{V=0} = \sqrt{Gi} \ln[(T - T_c)/T_c]$ , where  $Gi = (1.6/(k_F l)^3)(T_c/E_F)$ ; A. Larkin and A. Varlamov, *Theory of Fluctuations in Superconductors* (Clarendon Press, Oxford, 2005).